Oligomer Approaches for Solid-State Dye-Sensitized Solar Cells Employing Polymer Electrolytes

ARTICLE *in* THE JOURNAL OF PHYSICAL CHEMISTRY C · APRIL 2007

Impact Factor: 4.77 · DOI: 10.1021/jp067621k

4 AUTHORS, INCLUDING:

Moon-Sung Kang
Sangmyung University
112 PUBLICATIONS **3,053** CITATIONS

SEE PROFILE

Jong Hak Kim
Yonsei University
284 PUBLICATIONS **4,194** CITATIONS

SEE PROFILE

Oligomer Approaches for Solid-State Dye-Sensitized Solar Cells Employing Polymer Electrolytes

Moon-Sung Kang,[†] Jong Hak Kim,[‡] Jongok Won,[§] and Yong Soo Kang*

Department of Chemical Engineering, Hanyang University, Seongdong-gu, Seoul 133-791, Korea, Energy Lab, Samsung SDI Corporate R&D Center, 428-5 Gongse-dong, Giheung-gu, Yongin-si, Gyeonggi-do 449-577, Korea, Department of Chemical Engineering, Yonsei University, Seoul 120-749, Korea, and Department of Applied Chemistry, Sejong University, Seoul 143-747, Korea

Received: November 16, 2006; In Final Form: January 31, 2007

Three different approaches utilizing oligomers, termed the "oligomer approaches", followed by in situ self-solidification, were applied successfully to prepare solid-state dye-sensitized solar cells. The oligomer approach employs (1) supramolecules containing quadruple hydrogen-bonding sites at both chain ends, (2) oligomer blends with high-molecular-weight polymers, and (3) nanocomposites of oligomer with SiO_2 nanoparticles. The overall energy conversion efficiency was as high as 4.5% at 1 sun condition, which may be primarily due to both the increased ionic conductivity and the better interfacial contact between the TiO_2 layer and the electrolyte due to the deep penetration of the small-sized liquid oligomer electrolyte. A threshold ionic conductivity of $\sim 1 \times 10^{-4}$ S cm^{-1} was also observed, below which the ionic conductivity may play a key role in determining the photocurrent and the energy conversion efficiency. Above the threshold ionic conductivity, the ionic conductivity may play a less-important role and other factors such as the recombination of the electrons on the surface of the TiO_2 layer with I_3^- in the electrolyte and the charge-transfer resistance at the interface between the counter electrode and the electrolyte may be critical. The effect of chemical properties of the oligomer terminal groups was also investigated to determine that the methyl terminal group is the best among -OH, -NH_2, and -COOH primarily due to the least amount of change in the flat band potential.

Introduction

Dye-sensitized solar cells (DSSCs) based on a mesoscopic oxide semiconductor layer and dye sensitizer have attracted considerable interest in the past few decades because of attractive features such as their high-energy conversion efficiency and low production cost.[1−3] DSSCs typically comprise a nanocrystalline TiO_2 layer, which is placed in contact with an electrolyte containing redox couples such as I^-/I_3^- dissolved in a solvent. The electrolyte is an important component in determining the photovoltaic properties of DSSCs as well as their durability. Liquid solvents such as acetonitrile and methoxy propionitrile have been employed commonly as media for dissolving redox couples (i.e., I^-/I_3^-), resulting in an energy conversion efficiency as high as 11.04% (at 1 sun).[4] However, DSSCs employing liquid electrolytes may suffer from drawbacks such as a potential leakage of liquid solvents and their permeation through sealants.[5−7] Therefore, research on solid polymer or quasi-solid electrolytes has become attractive for preparing solid-state DSSCs.[5−13]

Solid polymer electrolytes (SPEs) are formed when salts are dissolved in a polymer solvent containing polar ligands such as oxygen atoms in poly(ether)s, and are consequently ionically conductive and applicable to solid-state electrochemical devices.[14,15] The ionic conductivity of SPEs depends on the concentration and the mobility of the charge carrier, which are mostly associated with the interaction between cations and ligands in the polymer solvent and the chain mobility of the polymer, respectively. Poly(ethylene oxide) (PEO) has been most intensively studied as a polymer solvent for SPEs owing to its chemical stability and high solvating ability for salts.[14,15] However, the ionic conductivity needs to be improved for most electrochemical applications. Thus, there have been various approaches to enhance the ionic conductivity of PEO by utilizing noncrystalline PEO derivatives and also by adding nanoparticle fillers for preventing crystal formation.[5−7] Nonetheless, there have been several successful applications of SPEs for preparing solid-state DSSCs with high-energy conversion efficiencies.[16]

The ionic conductivity of a polymer electrolyte comprising poly(epichlorohydrin-*co*-ethylene oxide) with 9% and 0.9% (w/w) NaI and I_2, respectively, was reported to be 1.5×10^{-5} S cm^{-1}, resulting in a high overall energy conversion efficiency of 2.6% at 10 mW cm^{-2}, whereas the corresponding value for neat PEO (molecular weight (M_w) = 1 000 000 g/mol) was 1.65×10^{-6} S cm^{-1}.[5] Another approach for enhancing the conductivity of SPEs is the introduction of inorganic nanofillers to prevent crystal formation and, consequently, to enhance the mobility of redox couples.[5,6] For instance, nanocrystalline TiO_2 particles were introduced to PEO/LiI/I_2 electrolyte to prevent crystal formation of PEO, resulting in a high overall energy conversion of 4.2% at 65.6 mW cm^{-2}.[6] These results suggest that the ionic conductivity is an important factor in determining the overall energy conversion efficiency of solid-state DSSCs. In addition, the importance of the interfacial contact between polymer electrolyte and dyes has been demonstrated recently

* To whom correspondence should be addressed. Phone: +82-2-2220-2336. Fax: +82-2-2296-2969. E-mail: kangys@hanyang.ac.kr.
[†] Samsung SDI.
[‡] Yonsei University.
[§] Sejong University.

10.1021/jp067621k CCC: $37.00
Published on Web 03/15/2007

SCHEME 1: Schematic Drawing of Oligomer Approaches

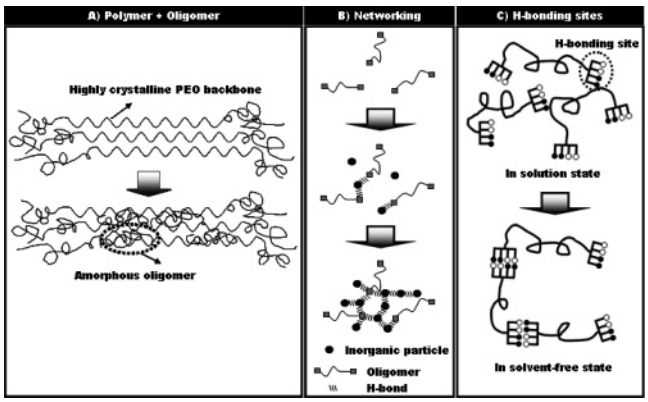

SCHEME 2: Poly(ethylene glycol) with [2-(6-Isocyanatohexylamino-carbonylamino)-6-methyl-4[1H]pyrimidinone] Terminal Groups (PHB)

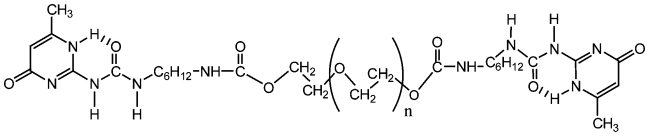

to utilize most dyes adsorbed on the TiO_2 surface for the improvement of the overall energy conversion efficiency.[8−10] That is, the deep penetration of electrolytes through the nanopores of the nanocrystalline TiO_2 layer is essential to provide better interfacial contact and, consequently, to obtain good photovoltaic performance.

Oligomers have been utilized successfully by a technique known as the "oligomer approach" to provide better interfacial contact between dyes and electrolytes as well as increased ionic conductivity for solid-state DSSCs, resulting in high-energy conversion efficiency.[8−10] Most oligomers are in the liquid state at ambient temperature with a M_w of ~1000 g/mol. To provide better interfacial contact, it is recommended that the pore size of the nanoporous TiO_2 layer be larger than the coil size of the oligomer. The average pore diameter of the typical nanoporous TiO_2 layer is in the range of 16 nm while the coil size of the poly(ethylene glycol) (PEG) oligomer with a M_w of 1000 g/mol in solution is less than 3 nm. Therefore, deep penetration of the oligomer-based electrolyte into the nanopores of the nanocrystalline TiO_2 layer is expected.

Because oligomer-based electrolytes are in the liquid state, solidification should be employed for preparing solid-state DSSCs. Recently, we have reported three different oligomer approaches for the preparation of solid-state DSSCs employing liquid oligomer-based electrolytes as shown in Scheme 1. The first approach was to utilize supramolecules of PEG oligomer (oligo-PEG, $M_w = 1000$ g/mol) having two quadruple hydrogen-bonding sites at both chain ends. It is a liquid during the cell fabrication procedure but becomes a solid polymer electrolyte with quadruple hydrogen bonds upon solvent evaporation. This solidification is referred to as in situ self-solidification. The molecular structure of the oligo-PEG having two quadruple hydrogen-bonding sites at both chain ends is shown in Scheme 2.[8] The overall energy conversion efficiency, η, was 3.34% at 1 sun and 1.5 AM conditions. Second, the use of an oligomer blend containing an amorphous liquid oligomer poly(propylene glycol) (oligo-PPG, $M_w = 750$ g/mol) with high-molecular-weight PEO ($M_w = 1$ M g/mol) also resulted in excellent photovoltaic performances (i.e., $\eta = 3.84\%$ at 1 sun and AM 1.5). Here, oligo-PPG played very important roles in both the deeper penetration of the electrolyte into the nanopores of the TiO_2 layer and the increased ionic conductivity by preventing crystal formation.[9] Third, low molecular poly(ethylene glycol) oligomer (oligo-PEG, $M_w = 500$ g/mol) based electrolytes have been solidified using fumed silica nanoparticles as a networking agent to become nanocomposites, resulting in a remarkably high-energy conversion efficiency of 4.5% at 1 sun (1.5 AM).[10] Therefore, the oligomer approach utilizing liquid oligomers, followed by in situ self-solidification for preparing solid-state DSSCs has been proven to be very effective in improving the energy conversion efficiency, primarily resulting from the enlarged interfacial contact between the dyes and the electrolyte and the increased ion conductivity.

In this article, the effect of the ionic conductivity and the interfacial contact on the photovoltaic characteristics of solid-state DSSCs was investigated systematically and elaborated in detail via the measurements of the flatband potential of photoelectrode, the ionic conductivity of electrolytes, and the incident photon to current conversion efficiency (IPCE). In particular, a threshold ionic conductivity of approximately 1×10^{-4} S cm^{-1} is obtained for 100 mW cm^{-2}, below which the ion transport through the bulk electrolyte appears to be a rate-determining step, but above which other factors than the ionic conductivity may also play an important role in determining the overall energy conversion efficiency.

Experimental Section

Electrolyte Preparation. Three different solid-state electrolytes were prepared according to the oligomer approach as described above. We have also prepared supramolecular electrolyte containing oligo-PEG ($M_w = 1000$ g/mol) with quadruple hydrogen-bonding sites, *X*I, and I_2 (here *X* is a cation). The mole ratio of oxygen atoms in the oligomer to iodide was fixed at 10:1 ([-O-]/[*X*I] = 10:1 with *X*I/I_2 = 10:1 w/w) because the ionic conductivity showed its maximum at this concentration. The detailed modification procedure was well-described in our previous paper.[8−10] The oligomer blend electrolyte was made by the blend of high-molecular-weight PEO ($M_w = 1$ M g/mol) and low-molecular-weight poly(propylene glycol) (oligo-PPG, $M_w = 425$ g/mol) or poly(ethylene glycol) dimethyl ether (oligo-PEGDME $M_w = 500$ g/mol) with a mole ratio of [-O-]/[*X*I] = 20:1 (here *X* is K or the 1-methyl-3-propylimidazolium cation) and *X*I/I_2 = 10:1 w/w. The blend ratio of PEO to oligomer was fixed at 4:6 (w/w). For the second approach, we prepared composite polymer electrolytes consisting of oligo-PEGDME/*X*I/I_2/fumed silica (amorphous, particle diameter of 20−30 nm, surface area of 255 ± 15 m^2 g^{-1}, and 3.5−4.5 OH groups μm^{-2}). The content of the silica nanoparticles was fixed at 9 wt % of the total polymer electrolyte, and the mole ratio of the oxygen atoms in the oligomer to iodide was fixed at 20:1 ([-O-]/[*X*I] = 20:1 with *X*I/I_2 = 10:1 w/w). Acetonitrile was employed as a solvent for the all-electrolyte solutions. All chemicals except imidazolium iodide were purchased from Aldrich. Imidazolium iodide (MPII, 1-methyl-3-propylimidazolium iodide) was obtained from Solaronix (Switzerland). The purities of the chemicals employed in this work were higher than 99.9%, and we have utilized them without further purification.

DSSC Fabrication. DSSCs were fabricated according to the following procedure. Transparent SnO_2/F-layered conductive glass (FTO, purchased from Pilkington. Co. Ltd., 8 Ω/□) was employed to prepare both the photo- and counter-electrodes. For the photoelectrode, a Ti(IV) bis(ethyl acetoacetato)-diisopropoxide solution (2% w/w in 1-butanol, Aldrich) was first

spin-coated onto FTO glass and then the glass was heated stepwise to 450 °C and maintained at this temperature for 20 min. Then, commercialized TiO_2 paste (Ti-Nanoxide T, Solaronix) was cast onto the FTO glass by a doctor-blade technique and successive sintering at 450 °C for 30 min. The nanocrystalline TiO_2 film (with a thickness of ca. 13−18 μm) was sensitized overnight with a $Ru(dcbpy)_2(NCS)_2$ dye (dcbpy = 2,2′-bipyridyl-4,4′-dicarboxylato) solution (535-bisTBA, Solaronix, 13 mg dissolved in distilled ethanol (50 g)). Pt-layered counter-electrodes were prepared by spin-coating of a H_2PtCl_6 solution (0.05 mol dm^{-3} in isopropanol, Aldrich) onto FTO glass and then successive sintering at 400 °C for 30 min. For solar cell fabrication, a dilute polymer electrolyte solution was first cast onto a dye-adsorbed TiO_2 electrode and evaporated very slowly for easy penetration of electrolytes through the nanopores of the TiO_2 layer. Next, a highly concentrated polymer electrolyte solution was cast onto the photoelectrode to minimize the time for evaporation of solvent as well as to prevent the formation of cavities between the two electrodes during the solvent evaporation. Then, both electrodes were superposed together and then pressed between two glass plates in order to achieve slow evaporation of solvent as well as to obtain a very thin SPE layer. The cells were placed in a vacuum oven for the complete evaporation of solvent for 1 day and then sealed with an epoxy resin.

Morphological Characterization. Morphological characterization for the nanocrystalline TiO_2 layer was carried out using a field-emission scanning electron microscope (FE-SEM, S-4700, Hitachi). The specific surface areas and average pore size distributions were obtained by the Brunauer−Emmett−Teller (BET) method.[17]

Ionic Conductivity and Solar Cell Efficiency. Ionic conductivity was measured using a lab-made four-point probe conductivity cell connected to an impedance analyzer (IM6, ZAHNER). The photoelectrochemical performance characteristics (short-circuit current J_{sc} (mA cm^{-2}), open-circuit voltage V_{oc} (V), fill factor *ff*, and overall energy conversion efficiency η were measured using a Keithley Model 2400 and a 1000 W xenon lamp (Oriel, 91193). The light was homogeneous up to an 8 × 8 in^2 area, and its intensity (or radiant power) was calibrated with a Si solar cell (Fraunhofer Institute for Solar Energy System, Mono-Si+KG filter, Certificate No. C-ISE269) for 1 sun light intensity (100 mW cm^{-2}), which was double-checked with a NREL-calibrated Si solar cell (PV Measurements Inc.). An increase in temperature inside the cell during measurement was prevented by using a cooler with a propeller. The cell performances were evaluated after vacuum drying for more than 10 days without any special sealing.

IPCE. IPCE was measured as a function of wavelength from 360 to 800 nm (PV Measurement Inc.) using a halogen source as monochromatic light and a broadband bias light for approximating 1 sun light intensity. The IPCE is defined by

$$IPCE = \frac{(1240[\text{eV·nm}]) \times (\textit{photocurrent density}[\mu\text{A·cm}^{-2}])}{(\lambda[\text{nm}]) \times (\textit{irradiance}[\mu\text{W·cm}^{-2}])} \quad (1)$$

Flatband Potential. Flatband potentials of photoelectrodes in the presence of oligomers with different terminal groups were monitored using an electrochemical cell system. An Ag/AgCl reference electrode, a platinum-wire counter electrode, a UV−vis spectrophotometer (8453, Agilent), and a potentiostat/galvanostat were used for measuring the flatband potential of the TiO_2-layered photoelectrodes (effective area = 0.5 cm^2).[18]

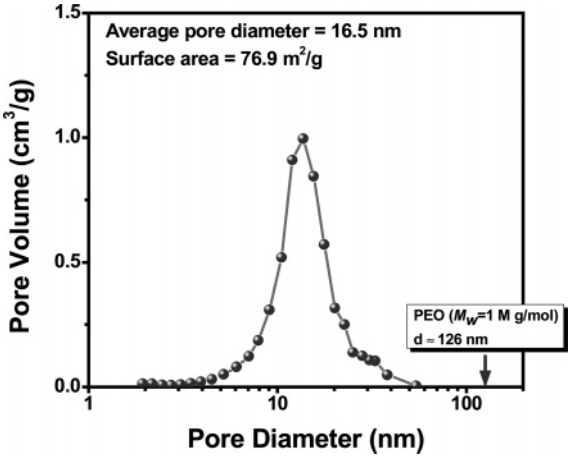

Figure 1. Pore size distribution of the nanocrystalline TiO_2 layer determined by BET measurement.

The supporting electrolyte solution was 0.5 M $LiClO_4$/ 0.2 M tetrabutyl ammonium perchlorate dissolved in CH_3CN with an oligomer content of 2.5% w/w.

Results and Discussion

Interfacial Contact between Dye-Adsorbed TiO_2 Nanoparticles and Electrolytes. The pore size distribution of the nanocrystalline TiO_2 layer determined from BET analysis is shown in Figure 1. The average pore diameter of the TiO_2 layer obtained from the N_2-desorption isotherm using the Barrett−Joyner−Halenda (BJH) method was approximately 16.5 nm, and the average surface area was 76.9 m^2 g^{-1}. The coil size of polymer chains in a good solvent can be represented by the radius of gyration, R_g, expressed by[19]

$$R_g = C(M_w)^{0.5} \quad (2)$$

where M_w is the molecular weight in g/mol and $C = 0.063$ (nm/(g/mol)$^{1/2}$)) for PEO. The R_g of high-molecular-weight PEO (i.e., M_w = 1 M g/mol) is 63 nm, and therefore the PEO coil may not readily penetrate into the nanopores of the TiO_2 layer due to the size difference. The cross-sectional FE-SEM image (the figure is not shown) shows a clear distinction between the TiO_2 layer and the electrolyte layer, suggesting that the polymer electrolyte solution hardly penetrated through the nanopores of the TiO_2 layer but instead accumulated onto the top of the TiO_2 layer. We also took cross-sectional FE-SEM images (Figure 2) for various molecular weights of PEO to confirm the dependence of the polymer coil size on the penetration behavior. When M_w = 1000 (1 K) g/mol, the TiO_2 particles were completely covered by the electrolyte solution, and their shape was not apparent but smooth, indicating deep penetration of the electrolyte into the nanopores. As the M_w of PEO increased, the TiO_2 particles had a more distinctive, original shape due to the poor penetration of the higher M_w polymer with larger coils. This shows the role of the coil size, that is, M_w of polymers, for better penetration into TiO_2 nanopores and, consequently, excellent interfacial contact between dye molecules and electrolytes. On the basis of these observations, it is recommended that the coil size of the electrolyte medium be smaller than the average pore diameter of the nanopores of the TiO_2 layer of 16.5 nm to achieve the deep penetration of electrolyte solution through the nanopores for better interfacial contact. In the case of PEO (or PEO derivatives), a molecular weight less than several thousands (especially under M_w = 2000 g/mol (R_g = 2.82 nm)) is recommended.

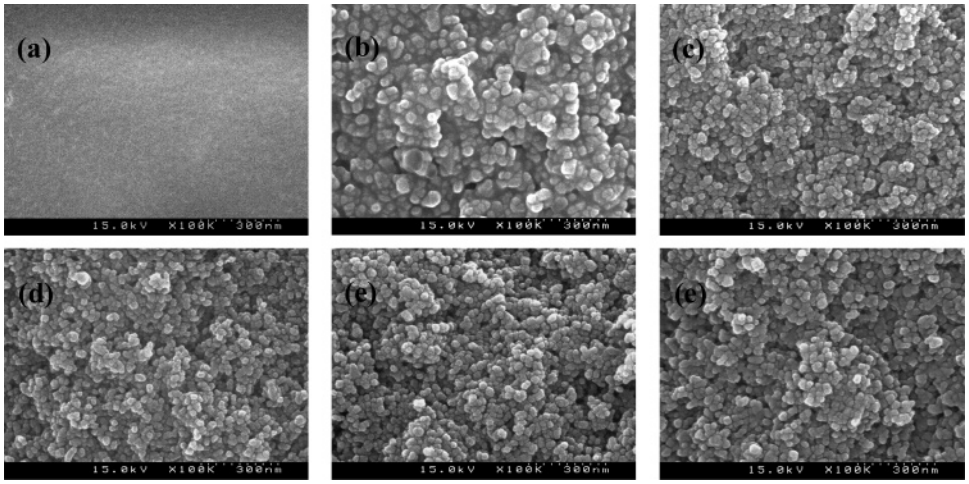

Figure 2. Cross-sectional FE-SEM images displaying the dependence of the penetration behavior on polymer (PEO) coil size: (a) $M_w = 1$ K g/mol ($R_g = 2.0$ nm), (b) $M_w = 4.6$ K g/mol ($R_g = 4.3$ nm), (c) $M_w = 8$ K g/mol ($R_g = 5.6$ nm), (d) $M_w = 10$ K g/mol ($R_g = 6.3$ nm), (e) $M_w = 100$ K g/mol ($R_g = 19.9$ nm), and (f) $M_w = 600$ K g/mol ($R_g = 48.8$ nm).

Ionic Conductivity (σ) and Shear Modulus. The ionic conductivity for PHB supramolecular electrolytes increased up to 5.28×10^{-5} S cm^{-1}, whereas that for neat PEO ($M_w = 1$ M g/mol) was 1.66×10^{-6} S cm^{-1}. The ionic conductivity of oligo-PEG/PEO blends increased almost linearly with the concentration of the oligomer as shown in Figure 3a. The higher ionic conductivity was primarily due to the increased chain mobility of the oligomers and also the prevention of crystal formation of PEO as evidenced by WAXS and DSC.[9] In the case of the nanocomposite of oligo-PEG/silica, the ionic conductivity increased with the content of the silica nanoparticles reaching a maximum followed by a decrease (as shown in Figure 3b). The silica nanoparticles may play important roles in increasing the ionic conductivity, mostly due to the generation of free volume at the interphase, as well as in solidifying the liquid oligomers by interaction forces among the silica particles.[20] These results suggest that the three oligomer-based electrolytes increased the ionic conductivity to some extent.

The shear modulus and viscosity of the supramolecular electrolyte were measured (Physica MCR 300 with $d = 1$ mm at a shear rate of 1/s) and plotted as a function of temperature as shown in Figure 4. Both shear modulus and viscosity increased slowly with temperature up to around 90 °C, followed by sudden drops. This suggests that the initial solid state change to liquid state at around 90 °C was presumably due to the breakage of hydrogen bonds between chain ends.

Terminal Functional Groups and Flatband Potential (V_{Fb}). Because oligomers have an abundant number of terminal functional groups owing to their short chain length, the reactivity of terminal functional groups of oligomers can significantly affect photovoltaic properties of DSSCs. Therefore, we investigated the effect of the terminal functional group of oligomers on the TiO_2/electrolyte interface by measuring the flatband potentials of the photoelectrode. The terminal groups investigated were -CH_3, -OH, -NH_2, and -COOH, and the content of the oligomers in the supporting electrolytes was fixed at 2.5% w/w. We utilized oligomers having similar molecular weights of 400−500 g/mol to ignore the influence of the molecular size on the flatband potential of DSSCs. The flatband potentials, V_{Fb}, measured by an absorption spectroscopic method,[18] are summarized in Table 1. The V_{Fb} values of the photoelectrode are largely dependent upon the characteristics of the terminal groups of the oligomers. Among the oligomers considered, the smallest change in the V_{Fb} value (i.e., +0.1 V vs Ag/Ag$^+$) was observed in the electrolyte solution of PEG containing CH_3 groups, whereas PEG containing carboxylic acids resulted in a large flatband potential shift (i.e., +0.86 V vs Ag/Ag$^+$). The change in the flatband potential results in the reduction of the

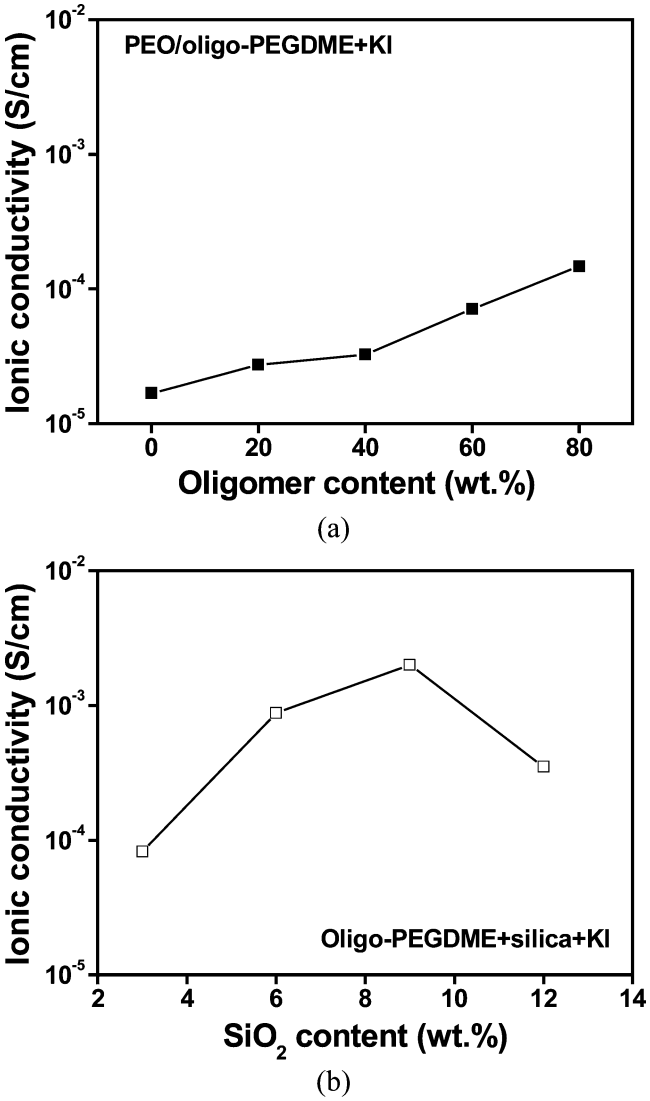

Figure 3. Ionic conductivities for solid-state polymer electrolytes: (a) PEO/oligo-PEGDME+KI and (b) oligo-PEGDME+silica+KI oligomer based electrolytes ([-O-]/[KI] = 20:1 mole ratio, KI/I_2 = 10:1 w/w).

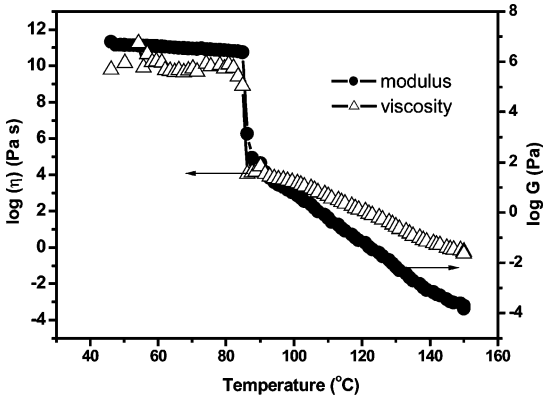

Figure 4. Modulus and viscosity of the PHB/IL electrolyte as a function of temperature.

TABLE 1: Flatband Potential of the TiO_2 Electrode in Various Electrolyte Solutions with or without Oligomer Additives (0.2 M $LiClO_4$/acetonitrile/oligomer Additive)

additives	flatband potential (V)
no additives	−1.20
poly(ethylene glycol) dimethyl ether (PEGDME)	−1.10
poly(ethylene glycol) (PEG)	−0.67
poly(propylene glycol) (PPG)	−0.70
poly(ethylene glycol) bis(carboxylmethyl) ether (PEGCME)	−0.34
poly(propylene glycol) diamine (PPGDA)	−0.99
PHB[a]	−0.69

[a] PHB = poly(ethylene glycol) with hydrogen-bonding end groups.

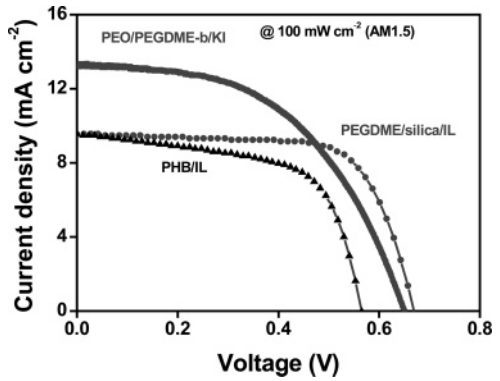

Figure 5. $J-V$ curves of DSSCs employing oligomer-based composite electrolytes ([-O-]/[XI] = 20:1 mole ratio, XI/I_2 = 10:1 w/w where X = K or 1-methyl-3-propylimidazolium) measured at 100 mW cm^{-2} illumination.

open-circuit voltage by decreasing the quasi-Fermi level of TiO_2 layer.[18,21] Consequently, it is believed that the use of oligo-PEG containing inactive methyl groups is more effective in improving the energy conversion efficiency compared to the others in terms of the V_{oc} characteristic of DSSCs.

Photovoltaic Properties. Figure 5 shows the comparison of photovoltaic performances (measured at 100 mW cm^{-2}, AM 1.5) of DSSCs employing oligomer-based electrolytes designed by means of the oligomer approach. The characteristics are summarized in Table 2. The solid-state DSSCs exhibited excellent photovoltaic performance with energy conversion efficiencies of η = 3.34%, 4.50%, and 4.42% at 1 sun, for PHB+MPII/I_2, PEGDME+Silica+MPII/I_2, and PEO_8PPG_2+MPII/I_2, respectively. These results show that the use of oligomers as an electrolyte medium followed by in situ self-solidification is very effective in preparing highly efficient solid-state DSSCs. In the

TABLE 2: Photovoltaic Characteristics of DSSCs Employing Oligomer-Based Composite Electrolytes ([-O-]/[XI] = 20:1 Mole Ratio, XI/I_2 = 10:1 w/w Where X = K or 1-Methyl-3-propylimidazolium)

SPE	Jsc (mA cm^{-2})	Voc (V)	ff (−)	η (%)
PHB[b]/IL	9.53	0.57	0.62	3.34
PEGDME/silica/IL[c]	9.58	0.67	0.70	4.50
PEO/PEGDME/KI	13.23	0.65	0.51	4.42

[a] Measured at 100 mW cm^{-2} (1 sun, 1.5 AM). [b] PHB = poly(ethylene glycol) with hydrogen-bonding end-groups. [c] IL = ionic liquid (MPII; 1-methyl-3-propylimidazolium iodide).

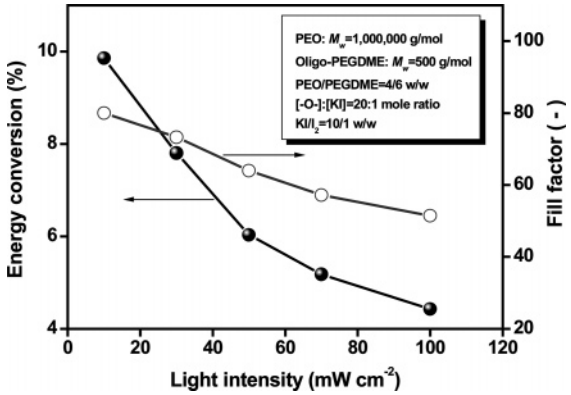

Figure 6. Effect of illumination intensity on the photovoltaic performances of DSSCs employing PEO+oligomer (PEGDME, M_w = 500 g/mol) composite electrolytes ([-O-]/[KI] = 20:1 mole ratio, KI/I_2 = 10:1 w/w).

case of DSSCs employing PHB electrolyte, a relatively low V_{oc} characteristic was observed owing to the significant change in V_{Fb} as shown in Table 1 (i.e., under Fermi level pinning, $V_{oc} = |V_{Fb} - V_{red}|$, where V_{red} is the standard reduction potential of the redox couple).[18,21]

The characteristic values (i.e., η and ff) for the oligomer blend electrolytes are plotted with variation of the illumination intensity in Figure 6. J_{sc} of 13.23 mA cm^{-2}, V_{oc} of 0.65 V, ff of 51%, and η of 4.42% at 1 sun were obtained even after vacuum drying for more than 7 days. FT−IR spectra also show the absence of volatile solvent (no C≡N stretching of acetonitrile at 2250 cm^{-1}, data not shown). In particular, the energy conversion efficiency was very high at around 10% at weak light intensity (i.e., 10 mW cm^{-2}). The significant difference of the energy conversion with variation in the light intensity might be caused by the ion transfer limitation occurring under strong incident light presumably owing to the retardation of ion diffusion in the highly viscous polymer medium and the high interfacial resistances at the electrode/electrolyte junctions. Fill factors were also shown to decrease with an increase in the illumination intensity. Nogueira et al. commented that the low conductivity of polymer electrolytes increases voltage losses arising from charge transport through the electrolyte (i.e., the series resistance of the cell) and such losses are most important for high current densities.[22] They also suggested that the low ion mobility presumably causes the generation of concentration gradients in the polymer electrolyte at high current densities. This ionic concentration gradient can promote the electron recombination reactions.

Figure 7 shows the IPCE spectra for solid-state DSSCs employing oligomer-based electrolytes. For DSSCs employing both the PEGDME+Silica+MPII/I_2 and PHB+MPII/I_2 electrolytes, IPCE values as high as approximately 60% were obtained at 530 nm, which are comparable to those typically observed for DSSCs employing gel or polymer electrolytes.[23]

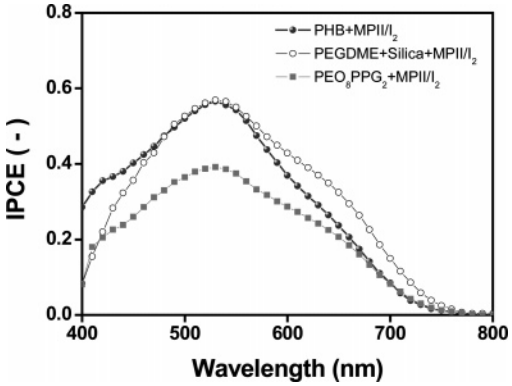

Figure 7. IPCE spectra of DSSCs employing solidified oligomer electrolytes based on high-molecular-weight PEO (M_w = 1 M g/mol) and oligomers (PEGDME, M_w = 500 g/mol; PPG, M_w = 425 g/mol) ([-O-]/[*X*I] = 20:1 mole ratio, *X*I/I_2 = 10:1 w/w where *X* = 1-methyl-3-propylimidazolium).

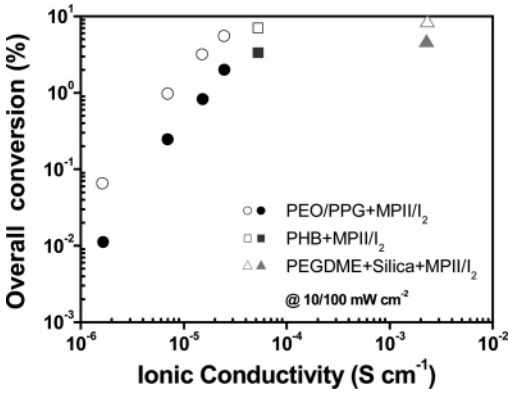

Figure 8. Relationship between overall energy conversion (η) and ionic conductivity (σ) of oligomer-based composite electrolytes ([-O-]/[*X*I] = 20:1 mole ratio, *X*I/I_2 = 10:1 w/w, here *X* = 1-methyl-3-propylimidazolium) (open symbols (○, □, △) are the data measured at 0.1 sun; close symbols (●, ■, ▲) are the data measured at 1 sun).

Moreover, the photocurrent action spectrum matched the IPCE characteristics of the $Ru(dcbpy)_2(NCS)_2$ dye well and it goes to zero at long wavelengths (>850 nm).[24] However, the DSSC employing high M_w PEO based electrolyte (i.e., PEO_8PPG_2+MPII/I_2) exhibited a relatively poor IPCE (40% at 530 nm), indicating that the insufficient penetration of electrolyte medium through TiO_2 nanopores limits the conversion of incident photons to electrons owing to the inferior interfacial contact between dye and electrolyte.

Threshold Ionic Conductivity. It has been understood that low ionic conductivity is a crucial factor in lowering the short circuit current and, consequently, the low overall energy conversion efficiency in solid-state DSSCs. If so, then it is interesting to determine a critical or threshold ionic conductivity, below which the ionic conductivity is a critical factor or the rate determining step in determining the short circuit current and, consequently, the overall energy conversion efficiency, but above which parameters other than the ionic conductivity may also play important roles.

Figure 8 shows the log−log relationship between the overall energy conversion efficiency and the ionic conductivity of oligomer-based electrolytes. The log overall energy conversion efficiencies increased almost linearly with an increase in the log ionic conductivity up to 1×10^{-4} S cm^{-1}, above which the energy conversion efficiency reached a plateau or at least increased with a much lower slope. This behavior was almost identical with that of the photocurrent. There is no significant difference in the ionic conductivity threshold measured at different illumination intensities. It seems that the ionic conductivity threshold is valid in the typical range of illumination intensity (i.e., 10−100 mW cm^{-2}). This reveals that the ionic conductivity in solid-state DSSCs could be a rate-determining step in determining the photocurrent and the overall energy conversion efficiency at ionic conductivities lower than the threshold ionic conductivity of 1×10^{-4} S cm^{-1}. Alternatively, at ionic conductivities higher than the threshold ionic conductivity, factors other than the ionic conductivity could play an important role in determining the photocurrent and the overall energy conversion efficiency. Note that DSSCs employing oligomer-based electrolytes exhibited almost the same V_{oc} values regardless of the ionic conductivities except for the PHB supramolecular electrolyte. The low V_{oc} value for the PHB supramolecular electrolyte is mostly due to the shift in the flat band potential as described previously, suggesting that it depends on the nature of the terminal functional groups of the oligomers, but not the ionic conductivity.

These results suggest that, in addition to the high ionic conductivity of the electrolyte for solid-state DSSCs, other factors such as the recombination and the interfacial resistances at the junction of electrolyte and electrode could be important in improving the overall energy conversion efficiency. For example, the modification of conventional Pt-layered counter-electrodes with various junction materials could reduce the interfacial electron-transfer resistance and, consequently, significantly enhance the overall conversion efficiency of solid-state DSSCs (the data are not shown). In summary, strategies to prepare highly efficient SPE-DSSCs can be categorized as (1) development of polymer electrolytes with high ionic conductivity and transport number for redox couples (i.e., I^-/I_3^-), (2) control of the coil size of polymer electrolytes for better interfacial contact between dye molecules and electrolytes, (3) prevention of electron recombination, and (4) development of counter-electrodes having low interfacial resistance for electron transfer between Pt catalysts and polymer electrolytes.

Conclusions

The oligomer approach based on liquid oligomer electrolytes, followed by in situ self-solidification, was applied successfully to prepare solid-state DSSCs having high overall energy conversion efficiencies as high as 4.5% at 100 mW cm^{-2} and AM 1.5. The improved efficiency was primarily due to the better interfacial contact between dyes and electrolytes by the deeper penetration of smaller-sized oligomer electrolytes through nanopores of the TiO_2 layer and the increased ionic conductivity. A threshold ionic conductivity in the range of 1×10^{-4} S cm^{-1} was observed, below which the ionic conductivity primarily dictates the photocurrent and, consequently, the energy conversion efficiency, and above which other important parameters than the ionic conductivity such as the recombination and the charge-transfer resistance at the counter electrode side also play important roles in determining the photocurrent and the energy conversion efficiency. It is also interesting that the methyl terminal group was the best among methyl, hydroxyl, amine, and carboxylic acid groups in terms of resulting in the least amount of change in the flat band potential, giving the highest energy conversion efficiency.

References and Notes

(1) O'Regan, B.; Grätzel, M. *Nature* **1991**, *353*, 737.
(2) Hara, K.; Sato, T.; Katoh, R.; Furube, A.; Ohga, Y.; Shinpo, A.; Suga, S.; Sayama, K.; Sugihara, H.; Arakawa, H. *J. Phys. Chem. B* **2003**, *107*, 597.

(3) Ferrere, S.; Gregg., B. A. *J. Phys. Chem. B* **2001**, *105*, 7602.
(4) Grätzel, M. *J. Photochem. Photobiol., A* **2004**, *164*, 3.
(5) Nogueira, A. F.; Durrant, J. R.; De, Paoli, M.-A. *Adv. Mater*. **2001**, *13*, 826.
(6) Stergiopoulos, T.; Arabatzis, I. M.; Katsaros, G.; Falaras, P. *Nano Lett.* **2002**, *2*, 1259.
(7) Katsaros, G.; Stergiopoulos, T.; Arabatzis, I. M.; Papadokostaki, K. G.; Falaras, P. *J. Photochem. Photobiol., A* **2002**, *149*, 191.
(8) Kim, Y. J.; Kim, J. H.; Kang, M.-S.; Lee, M. J.; Won, J.; Lee, J. C.; Kang, Y. S. *Adv. Mater.* **2004**, *16*, 1753.
(9) Kang, M.-S.; Kim, J. H.; Kim, Y. J.; Won, J.; Park, N.-G.; Kang, Y. S. *Chem. Commun.* **2005**, 889.
(10) Kim, J. H.; Kang, M.-S.; Kim, Y. J.; Won, J.; Park, N.-G.; Kang, Y. S. *Chem. Commun.* **2004**, 1662
(11) Kubo, W.; Kitamura, T.; Hanabusa, K.; Wada, Y.; Yanagida, S. *Chem. Commun.* **2002**, 374.
(12) Wang, P.; Zakeeruddin, S. M.; Exnar, I.; Grätzel, M. *Chem. Commun.* **2002**, 2972.
(13) Stathatos, E.; Lianos, P.; Lavrencic-Stangar, U.; Orel, B. *Adv. Mater.* **2002**, *14*, 354.
(14) Mao, G.; Perea, R. F.; Howells, W. S.; Price, D. L.; Saboungi, M. L. *Nature* **2000**, *405*, 163.
(15) Gadjourova, Z.; Andreev, Y. G.; Tunstall, D. P.; Bruce, P. G. *Nature* **2001**, *412*, 520.
(16) Li, B.; Wang, L.; Kang, B.; Qiu, Y. *Sol. Energy Mater. Sol. Cells* **2006**, *90*, 549.
(17) Brunauer, S.; Emmett, P. H.; Teller, E. *J. Am. Chem. Soc.* **1938**, *60*, 309.
(18) Kang, T.-S.; Chun, K.-H.; Hong, J. S.; Moon, S.-H.; Kim, K.-J. *J. Electrochem. Soc.* **2000**, *147*, 3049.
(19) Vandermiers, C.; Damman, P.; Dosière, M. *Polymer* **1998**, *39*, 5627.
(20) Merkel, T. C.; Freeman, B. D.; Spontak, R. J.; He, Z.; Pinnau, I.; Meakin, P.; Hill, A. J. *Science* **2002**, *296*, 519.
(21) Kang, M.-S.; Kim, Y. J.;Won, J.; Kang, Y. S. *Chem. Commun*. **2005**, 2686.
(22) Nogueira, A. F.; De Paoli, M.-A.; Montanari, I.; Monkhouse, R.; Nelson, J.; Durrant, J. R. *J. Phys. Chem. B* **2001**, *105*, 7517.
(23) Hara, K.; Sato, T.; Katoh, R.; Furube, A.; Ohga, Y.; Shinpo, A.; Suga, S.; Sayama, K.; Sugihara, H.; Arakawa, H. *J. Phys. Chem. B* **2003**, *107*, 597.
(24) Grätzel, M. *Prog. Photovoltaics* **2000**, *8*, 171.